On the Origin of Lifetime Extension for HMPE Ropes in Bending Operations

Marcel Meuwissen, Daniëlle Glasbergen, Michèl Kösters
DSM Ahead
Geleen, The Netherlands
marcel.meuwissen@dsm.com

Rigo Bosman, Paul Smeets, Hans Schneiders
DSM Dyneema
Urmond, The Netherlands

***Abstract*— Cyclic bending over sheave fatigue tests on braided ropes of high modulus polyethylene fibers were carried out for developing a better understanding of their failure. Damage accumulation at strand cross-over locations was identified as the main failure mechanism. At these locations, strands repetitively bend and slide over each other under high contact pressure. The application of a DSM proprietary finish termed XBO markedly improved the braid lifetime. This is attributed to the friction and adhesion lowering properties of the finish. The damage accumulation process in the filaments was studied in more detail in a filament friction test. This test showed that the filament gets damaged gradually over its whole volume and not only close to the contact surface.**

Keywords—synthetic fiber ropes; high modulus polyethylene filaments; bending fatigue; Dyneema® SK75 XBO

I. Introduction

High performance synthetic fiber ropes are increasingly being applied as replacement for steel wire ropes in commercial marine applications such as harbor towing, ship and offshore platform mooring, and (deep sea) lifting. The main advantages of synthetic fiber ropes are high strength and modulus, light weight, and ease of handling. The fiber materials in use on a commercial scale today are aramids, high modulus polyethylene, and liquid crystal polymers.

Fig. 1. Example of an application of a rope with Dyneema®: harbor towing on drum winch.

Dyneema® is a trademark of DSM. Use of this trademark is prohibited unless strictly authorized.

One of the potential failure mechanisms is rope breakage after repetitive bending and stretching, for example on winches and sheaves. In contrast to steel wire ropes, the amount of research on the bending performance of synthetic fibers is fairly limited. Nevertheless, studies for the most common synthetic high performance fiber materials are reported in literature: high modulus polyethylene fibers[3][9][19][20], aramid fibers[3][10][11], and liquid crystal polymer fibers[17].

This paper reports on experiments carried out on small scale braids of high modulus polyethylene fibers. Repetitive bending experiments were conducted under lab conditions. These experiments were aimed at improving the understanding of the mechanisms that eventually lead to rope failure. In addition, lab scale tests were carried out on single filaments for a more detailed study of the degradation mechanisms as encountered in ropes.

II. Cyclic Bending Tests on HMPE Braids

The bending performance of HMPE was investigated on small scale 12 strand braids (5 mm nominal diameter). Both standard filaments and filaments with an XBO finish were tested.

A. Test Set-Up

The cyclic bending over sheave test set-up is sketched in Fig. 2. Images of the set-up are shown in Fig. 3 and Fig. 4.

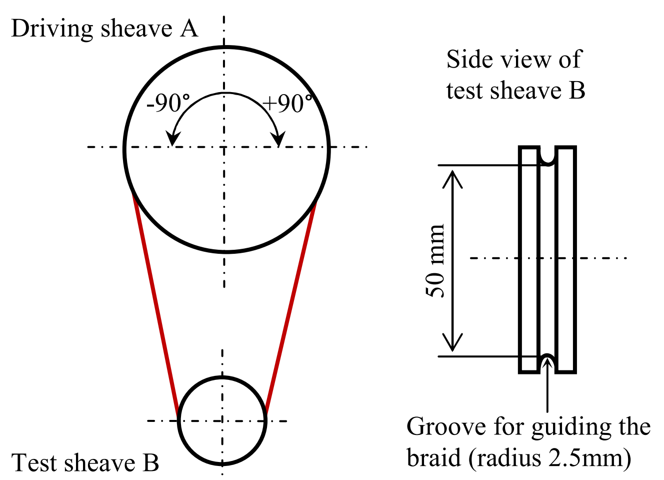

Fig. 2. Set-up used for performing bending fatigue experiments on small scale HMPE braids. The right panel shows a side view of the test sheave B.

978-0-933957-40-4 ©2013 MTS

This is a DRAFT. As such it may not be cited in other works. The citable Proceedings of the Conference will be published in IEEE Xplore shortly after the conclusion of the conference.

The main components in this set-up are a driving sheave (A) and a freely rotating test sheave (B). The braid is guided through a groove in the test sheave. This groove has a bottom radius of 2.5 mm. The nominal bending diameter of the braid on the test sheave B is 50 mm. The braid ends are fixed to pins mounted on the 300 mm diameter driving sheave (see Fig. 4). The braid is guided on this driving sheave through similar grooves as on the test sheave. An axial tensile force is applied on the braid by moving the test sheave B downwards. Both the total vertical force on the test sheave and the position of this sheave are logged during a test. The driving sheave rotates back and forth around its axis over ±90°. The sheave is driven by a motor and the required torque is logged by a torque cell installed between the motor and the sheave. The rotation of the driving sheave is logged as well.

Fig. 3. Overview image of the bending over sheave test set-up.

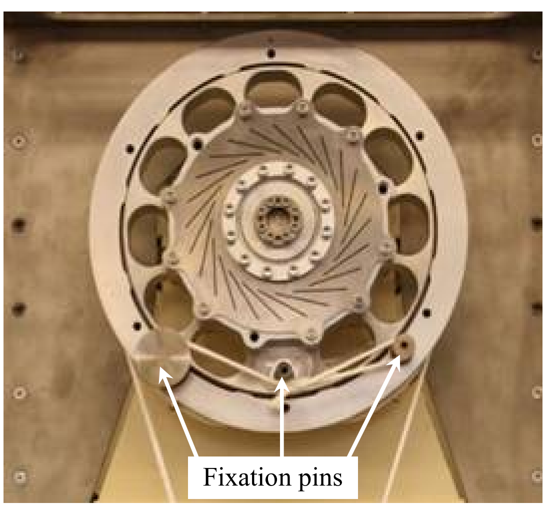

Fig. 4. Detailed image of the driving sheave A showing three pins used to fix one end of the braid. Three pins on the backside of this sheave (not visible in this image) are used to fix the other end of the braid.

Before starting a test, a fresh braid is guided through the groove on the test sheave, and the ends are fixed to the pins on each side of the driving sheave. Next, the braid is preloaded by 1.25 kN axial force. After unloading, the braid is fixed anew to the pins on the driving sheave to compensate for the setting elongation due to the preload. Next, the 1.25 kN pre-load is applied again and this force is gradually reduced to 0 N by moving the test sheave upwards. The position at zero vertical force is then taken as the reference position of the test sheave. Finally, the vertical load is increased to the set value (20% ABL) and the cycling is started. The end of life is defined as the cycle at which the braid breaks. The test parameters are summarized in TABLE I.

TABLE I. PARAMETERS FOR THE BENDING FATIGUE TESTS ON BRAIDS.

Parameter	Value
Construction	12 strands braided
Nominal braid diameter	5 mm
Axial load	4 kN (20%ABL)
Stroke angle driving sheave	±90°
Stroke length	500 mm
Ambient temperature	23°C
Relative humidity	50%
Cycle time	6 s

During the bending and stretching of the braid over the test sheave, filaments and strands slide over each other under high contact pressures (perpendicular to filament axis). The two sources for these pressures are: (i) contact pressure between strands due to the axial load on the braid, and (ii) contact pressure between the braid and the sheave. Because of the complexity of the braid construction, it is difficult to estimate the contact pressure due to the axial load. The contact pressure p_N between the braid and the test sheave is, to a first order approximation, estimated from:

$$p_N = \frac{2T_R}{D_S d_R}, \tag{1}$$

where T_R is the tensile force in the rope, D_S is the diameter of the test sheave and d_R is the diameter of the braid. Using the values for the current test set-up and braid, the contact pressure is estimated at 40 MPa.

B. *Braid Materials*

The bending tests are carried out on 12 strand braids made with SK75 fibers from DSM Dyneema. The main properties of the SK75fiber are given in TABLE II.

TABLE II. PROPERTIES OF SK75 FIBER FROM DSM DYNEEMA.

Property	Value
Tenacity	35.1 cN/dtex / 3.4 GPa
Modulus	1160 cN/dtex / 113 GPa
Elongation to breakage	3.5 %
Number of filaments in fiber	780
Filament linear density	2.3 dtex
Nominal filament diameter	17.4 µm

An SEM image of a standard SK75 filament is shown in the top panel of Fig. 5. The SK75 filaments have a nearly circular cross section. The filament diameter varies typically from about 16 µm to 19 µm. The particular surface structure introduced during the spinning and drawing processes is clearly visible.

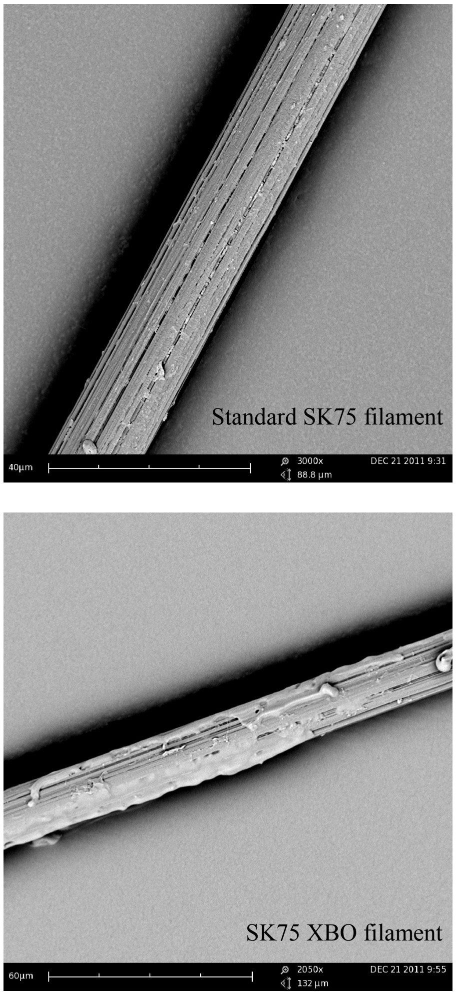

Fig. 5. Standard SK75 filament (top) and SK75 filament with XBO finish (bottom).

The bending performance of the standard SK75 filaments is compared to that of SK75 filaments with an additional XBO finish.

An SK75 filament with XBO finish is shown in the bottom panel of Fig. 5. The XBO finish is generally present on all filaments in a fiber.

C. Test Results

The lifetimes of standard braids and braids with XBO finish are compared in Fig. 6. The reported lifetimes are the averages of 3 tests. The error bars indicate a range equal to twice the standard deviation. Under the current test conditions, the finish increases the bending lifetime by a factor of 4.

Fig. 7 shows the downward displacement of the test sheave B (see Fig. 2) as a function of lifetime. This downward displacement partly compensates for elongation of the braid and partly for possible slip of the braids over the fixation pins and the driving sheave.

At the start of the experiment, the axial load is applied to the braid by moving the test sheave downwards. For the standard braids, this displacement is about 80 mm and for the braids with XBO finish it is about 110 mm.

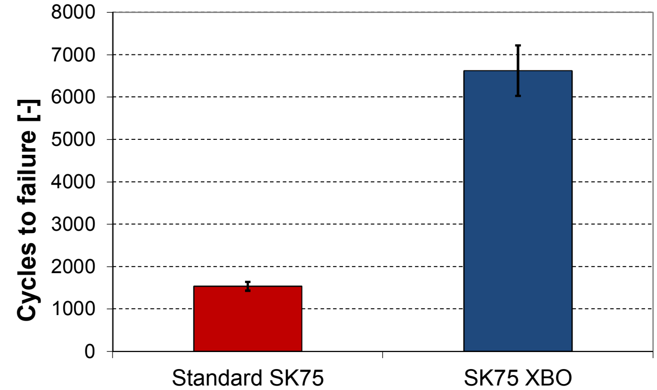

Fig. 6. Lifetime in cycles to failure for braids with standard SK75and braids with SK75 XBO.

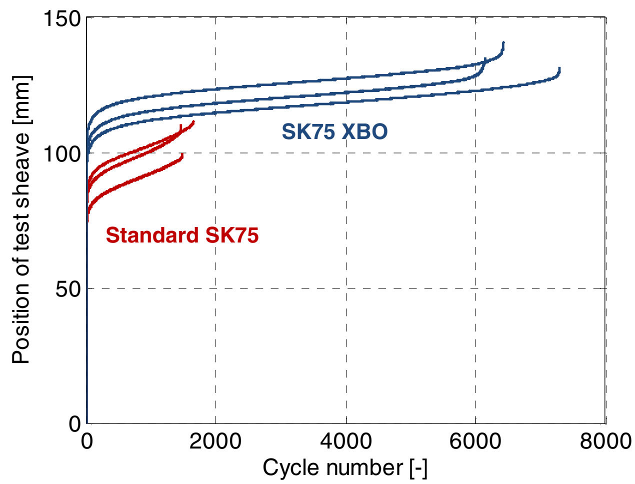

Fig. 7. Downward displacement of the test sheave B (see Fig. 2) as a function of time for bending tests on braids with standard SK75 and braids with SK75 XBO.

During the cycling, the total vertical force on the sheave is maintained at the set value (force required to maintain an axial force of 20% ABL in the braids) by moving the test sheave downwards. After a strong increase at the beginning of the fatigue test, the downward sheave displacement continues at a more or less constant rate for the majority of the experiment. Just before breakage, the elongation rate increases again.

Part of the sheave displacement compensates for braid elongation. This elongation could either be due to setting of the braid construction or due to creep straining of the filaments. It is believed that the setting of the braid construction occurs in the first few bending cycles and that the elongation after that is mainly due to creep strain in the filaments. It is remarkable that the elongation rate is different for the two braid types. Possible explanations for this difference are a different braid temperature (see below) or a different intrinsic creep rate due to different damage accumulation rates.

Two examples of the measured torque signal as a function of time are shown in Fig. 8. The torque signal is relatively constant over the lifetime and increases sharply in the last 50 to 100 cycles of the tests. The torque on the driving sheave is required to overcome losses: losses in the bending tester (such as the bearings) and losses in the braid (hysteresis, friction). Offline tests with elastic metal ribbons instead of braids have shown that, at 4 kN axial braid load, the torque required to overcome the losses in the bending tester itself is about 3 Nm.

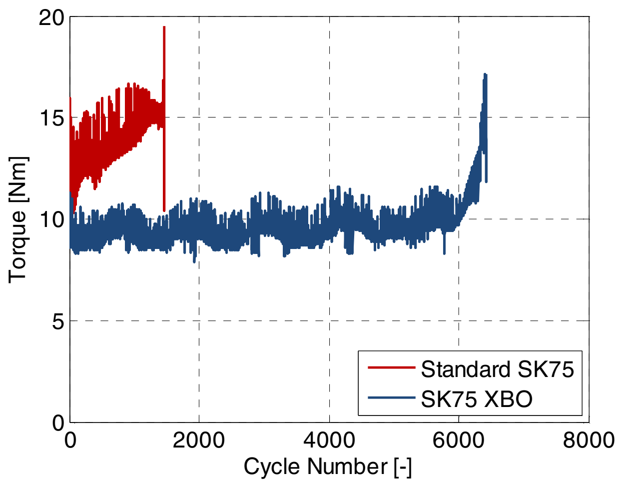

Fig. 8. Measured torque signal of the driving sheave as a function of time for the two types of 12 strand braids with SK75.

From the measured torque, the average dissipated energy per machine cycle can be calculated. This average dissipated energy is shown in Fig. 9 for the two braid types. The energy shown in this figure is corrected for losses in the bending tester. The energy dissipated in the standard braids is nearly twice of that dissipated in the braids with XBO finish.

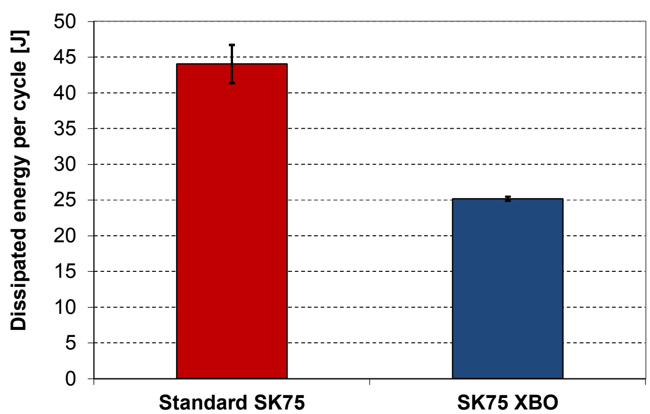

Fig. 9. Dissipated energy per machine cycle for the two types of 12 strand braids with SK75.

The dissipated energy is transformed into heat which will lead to an increase of braid temperature. As a first estimate of this temperature increase, it is assumed that all dissipated energy is taken up by the braid as heat i.e. the braid is fully isolated from the environment. Taking the specific heat capacity of PE as 1550 J/kgK, and 45 J heat dissipation (value measured for the standard braid), the (worst case) temperature increase for 0.5 m of braid (stroke length) is estimated at approximately 7°C per cycle. Because the heat can flow away to the environment (air and sheaves) during the test, the actual braid temperature increase is expected to be lower than this estimate.

Experiments have been carried out in which the temperature in the core of the braid is measured by a thermocouple. The measured temperature over the first few 100 cycles is shown in Fig. 10. The temperature could only be logged for a limited number of cycles because the thermocouples themselves are also fatigued during the test and fail prematurely. The temperature increase in the first few cycles is on the order of 5°C to 10°C which is in good agreement with the estimate above. The temperature increase is clearly much stronger for the standard braid which is in line with the observed higher amount of dissipated energy.

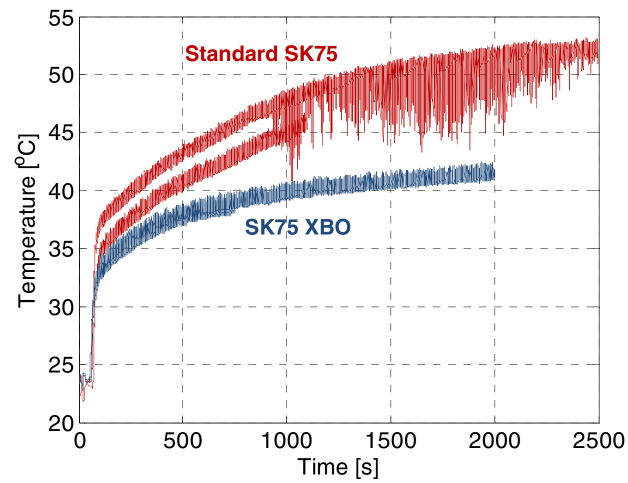

Fig. 10. Temperature as measured by thermocouples in the core of the braid for 2 experiments on braids standard SK75 and 2 experiments on braids with SK75 XBO.

After the first few cycles, the temperature increase slows down considerably. This temperature profile has also been witnessed in several real life tests of ropes with diameters of more than 100mm, confirming that ropes made with HMPE can be used in severe bending applications.

D. Braid Morphology

Fig. 11 shows the braid with XBO finish before the bending test (top) and at 90% of its lifetime (bottom). Compaction of the braid and broken filaments are clearly visible in the bottom image. The bending stiffness of the fatigued sample is much higher than that of the non-fatigued sample. The bending stiffness of a standard braid at 90% lifetime is even higher than that of a braid with XBO finish at 90% lifetime. This suggests that the interaction (adhesion) between the standard filaments is stronger than that between the filaments with XBO finish.

Cross sections of part of a standard SK75 braid and a braid with XBO finish at 90% of their lifetime are shown in Fig. 12. For the standard braid, 5 (parts of) strands can still be discerned. Some epoxy (used for sample preparation, light gray areas in Fig. 12) managed to penetrate into the cavities between the strands, but no epoxy can be seen in the interior of the strands. The adhesion between the filaments is strong enough to survive the handling during sample preparation and cross sectioning. This is in contrast with the cross section of the braid with XBO finish. Here, the epoxy managed to penetrate into the interior of the strands because of the weaker interaction between the filaments. These images are in line with the observed higher bending stiffness of the standard braids after the test.

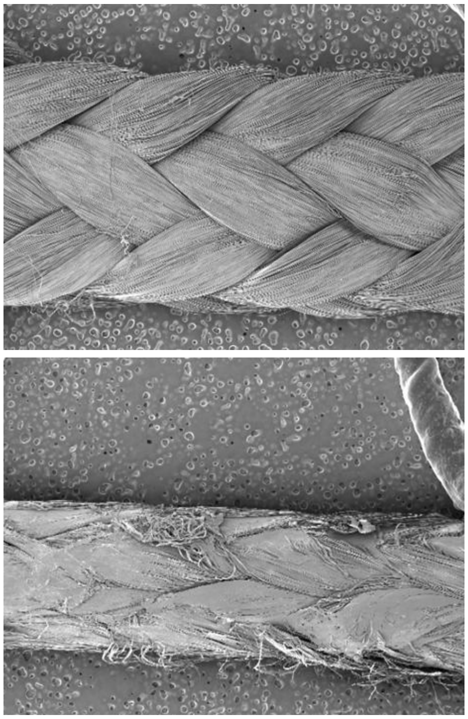

Fig. 11. SEM images of a braid with SK75 XBO before the test (top) and at 90% of its lifetime (bottom).

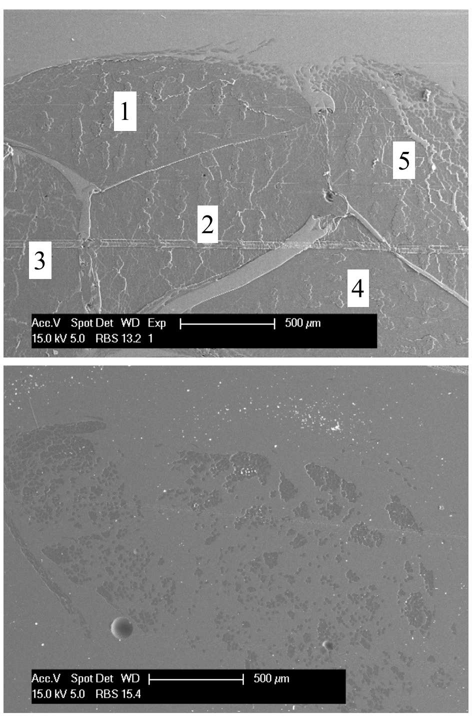

Fig. 12. SEM images of the cross section of a braid with standard SK75 (top, different strands are numbered) and a braid with SK75 XBO (bottom). Both braids are at 90% lifetime. The dark gray spots are cross sectioned filaments and the light gray domains are the areas of the epoxy.

E. *Braid and Filament Tenacity*

The tenacity of the braids as a function of lifetime is shown in Fig. 13. Bending fatigue tests were interrupted at different stages of the lifetime. Next, either the linear strength of the full braid was determined or the strength of single filaments. In the latter case, filaments were isolated from the braid and tested in a Favimat filament tensile tester[4]. The results of the filament tests might be biased due to the possible damage introduced during the isolation process, as it turned out to be difficult to isolate the filaments from the braids, in particular when the braids were near the end of their lifetime.

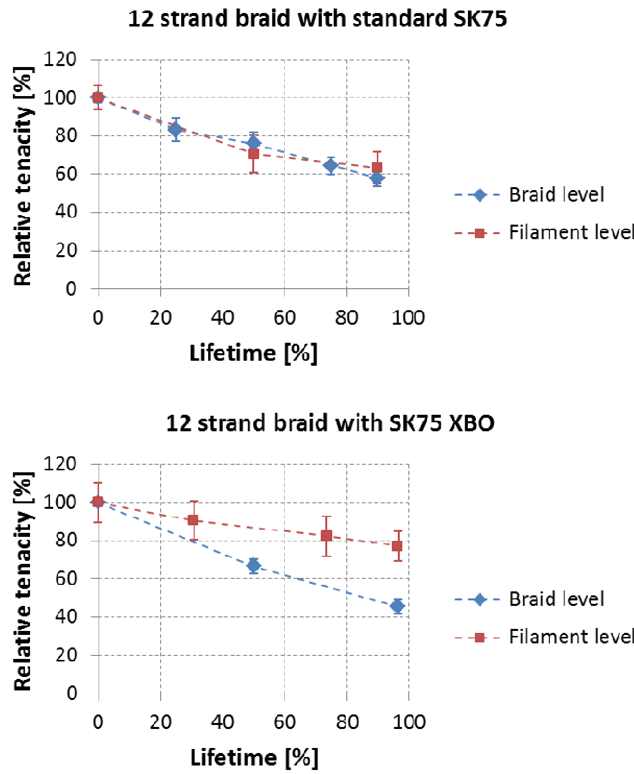

Fig. 13. Relative tenacity at braid and filament level for briads with standard SK75 (top) and braids with SK75 XBO (bottom).

For both braid types, the strength reduces gradually as a function of lifetime. A remarkable difference however is the rate at which strength decreases at filament and braid level. For the standard braids, this reduction occurs at the same rate whereas for the braids with XBO finish, the reduction is stronger at braid level than at filament level. This suggests a difference in (the balance of) the failure mechanisms.

F. *Hypothesis on Bending Fatigue*

The bending fatigue tests on braids have shown that the performance is significantly improved by proper surface modification of the filaments. It appears that in particular low friction and low adhesion between filaments improves bending performance. It is believed that for the current experiments, creep is not the main failure mechanism although some creep deformation occurs.

Fig. 14 graphically illustrates the current hypothesis on the mechanisms that lead to failure in repetitive bending.

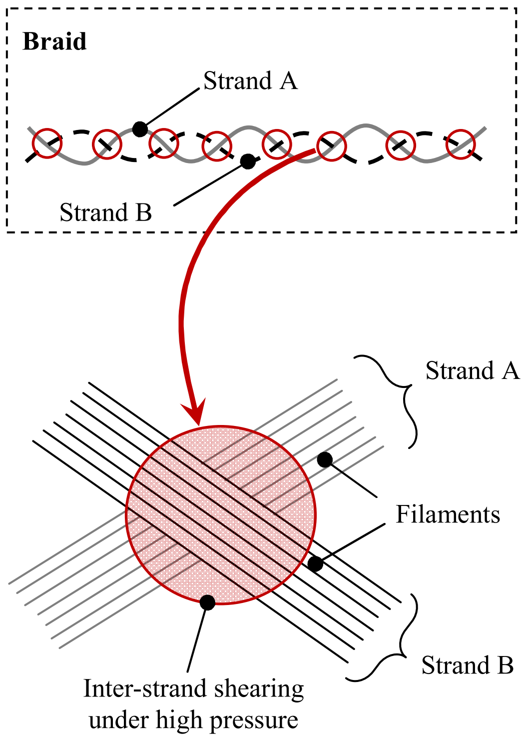

Fig. 14. Hypothesis on bending fatigue.

The strands in a braid cross each other at multiple locations (schematically indicated by red circles in the top panel of Fig. 14). During a bending cycle, the strands slide over each other and in particular at these cross-over locations this occurs under high normal pressure. Moreover, additional bending and stretching of strands over each other is also expected. This is deemed to be more detrimental than the overall bending of the full braid because the determining bending radius is that of the strand (typically less than 1 mm) instead of that of the sheave (25 mm). The cross section of the rope and strands are also continuously deformed leading to additional straining within each strand.

The main degradation mechanisms are inter-strand shearing and intra-strand shearing at cross-overs. The latter mechanism is probably stronger for filaments with stronger interaction such as the standard ones. Some evidence for this is found in the fact that all filaments taken from partly fatigued braids show a strong reduction of their tenacity whereas for braids with XBO finish, the tenacity at filament level is higher than that at braid level. The XBO lowers filament interaction (shearing) which reduces the damage driving forces.

The shearing of filaments over each other under high normal pressure is most likely the main driving factor for fatigue damage during bending cycling of braids. This process is studied in more detail with a dedicated experimental set-up described in the next section.

III. Filament Friction Test

Studying the wear mechanism of filaments sliding over each other in braids is quite complex, mainly due to the braid construction which makes it difficult to determine conditions under which the process is taking place, such as sliding distances, axial loading, and lateral loading. For these reasons, a filament friction test is considered here, which still captures the main characteristics of the bending test on a braid, but is more straightforward to analyze.

Friction tests on synthetic filaments have been addressed in literature over the past 50 years [1][2][7][12][14][15][16][18], but in most of these tests, the filament is sliding over a counter body of a different material or at relatively mild contact pressures.

A. *Test Set-Up*

The test set-up used here is shown in Fig. 15. A fiber is attached with one end to a pin on a fixture. It is guided over a second pin on the fixture and kept taut by a dead weight attached to the other end of the fiber (10 N). The test section of the fiber is in horizontal position. The fixture is installed on the upper traverse of a standard tensile tester.

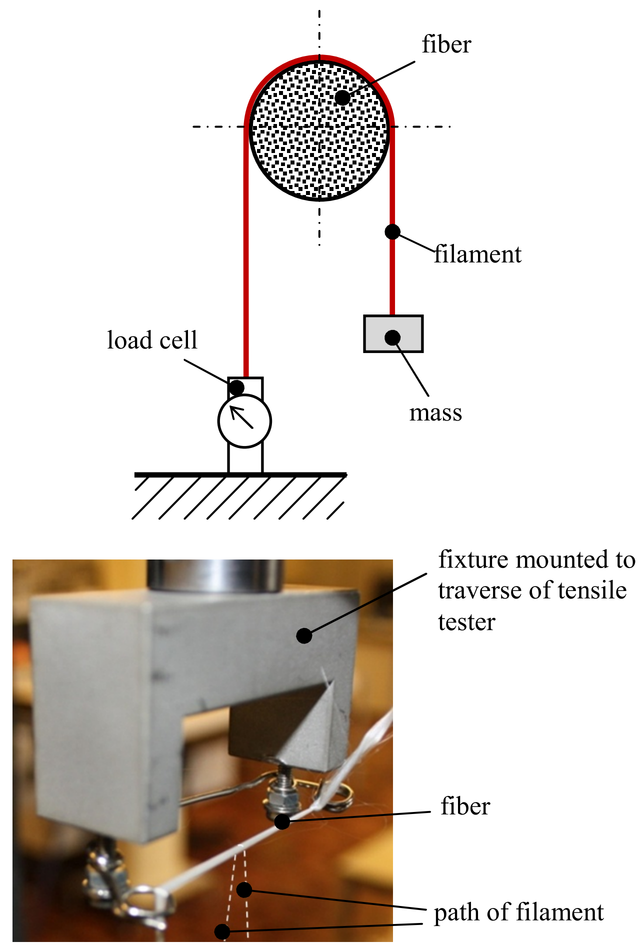

Fig. 15. Schematic drawing of filament friction test set-up (top) and image of the actual set-up (bottom). In the bottom panel, the path of the filament is indicated by the white dashed lines as the actual filament is not visible at this magnification.

A filament is slung over the test section of the fiber and fixed at one end to a load cell and at the other end to a dead weight. The upper traverse of the tensile tester is moved up and down causing the filament to slide back and forth over the fiber. The end of the test is defined as the cycle in which the sliding filament breaks.

The nominal settings for the test are summarized in TABLE III. The mass at one end of the filament is 12.8g, corresponding to a nominal axial tensile stress of 530 MPa which is approximately 15% of the tenacity of the filament. If there is no friction between the filament and the fiber, the tensile stress is constant over the length of the filament. If the contact width between the fiber and the filament is 30μm, the contact pressure is estimated at 17 MPa (see Appendix). This is lower but nevertheless on the same order of magnitude of the contact pressures occurring in the braid (see above).

TABLE III. NOMINAL SETTINGS FOR FILAMENT FRICTION TEST.

Parameter	Value
Fiber	1760 dtex SK75 (780 filaments)
Nominal fiber diameter	0.5 mm
Filament	2.3 dtex SK75
Nominal diameter filament	17.4 µm
Mass at end of filament	12.8 g
Sliding velocity of filament over fiber	1.7 mm/s
Stroke	10 mm
Cycle time	15 s

In the actual test, there is friction between the filament and the fiber. In that situation, the axial tensile force is no longer constant along the length of the filament and consequently the contact pressure will also vary (see Appendix).

B. Test Results

An example of a filament and fiber with XBO finish at 90% of the lifetime is shown in Fig. 16 and Fig. 17.

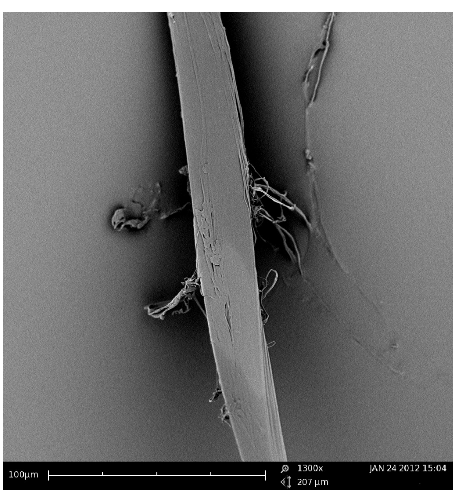

Fig. 16. Filament with XBO finish at 90% of the lifetime in the filament friction test.

The cross section of the filament has changed from the original nearly circular shape to a ribbon like shape. The width of the contact area is approximately 30µm. The surface of the filament that was in contact with the fiber is smoother than at the start of the experiment (compare Fig. 17 to Fig. 5). Some loose fibrils are visible as well, but on average, the amount of debris on the filament appears to be rather limited.

Fig. 17 shows part of the fiber that has been in contact with the filament. A wear 'track' slightly wider than the filament is clearly visible. Debris has accumulated at the boundaries of this track. The filaments at the surface of the fiber have been damaged as well due to the sliding action.

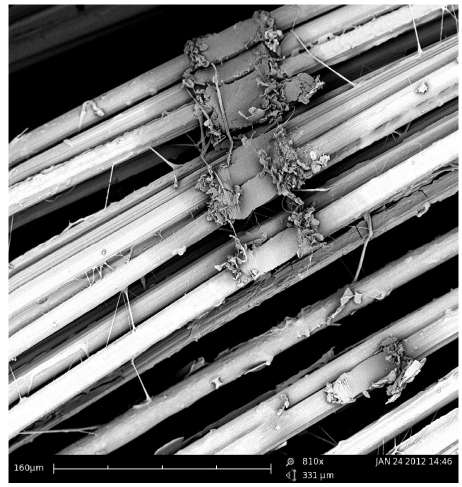

Fig. 17. Fiber with XBO finish at 90% of the lifetime in the filament friction test.

The average number of cycles to failure for the standard filaments and the filaments with XBO finish are shown in Fig. 18.

The scatter on the measurement results is quite high (see error bars in the figure). The scatter may be partly due to the variation in filament properties such as the diameter. Nevertheless, it is clear that the XBO coating increases the lifetime which is in agreement with the bending fatigue tests at braid level.

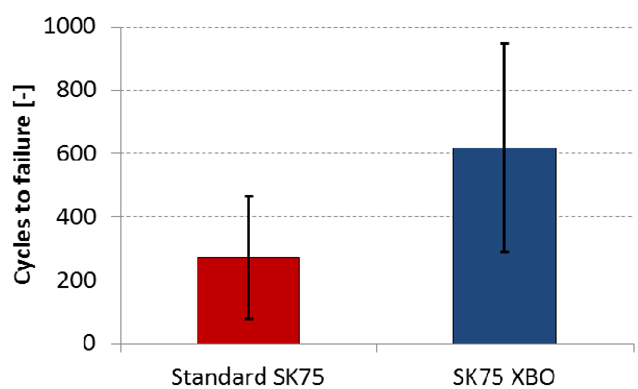

Fig. 18. Average number of cycles to failure in the filament friction test for standard SK75 and SK75 with XBO finish.

Two characteristic curves of the development of the coefficient of friction as a function of cycle number are shown in Fig. 19. The coefficient of friction at the start of the experiment is around 0.1 and gradually increases to nearly 0.3. The increase is steeper for the standard filaments.

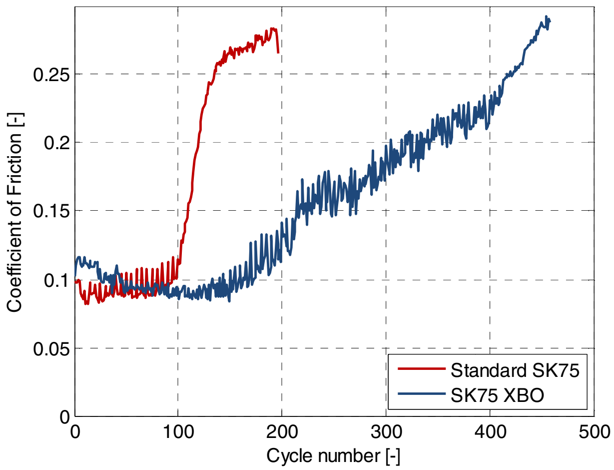

Fig. 19. Coefficient of friction for standard filaments sliding over standard fibers and filaments with XBO finish sliding over fibers with XBO finish.

The increase in coefficient of friction could be related to the increase in contact area between the sliding filament and the fiber. This is schematically explained in Fig. 20.

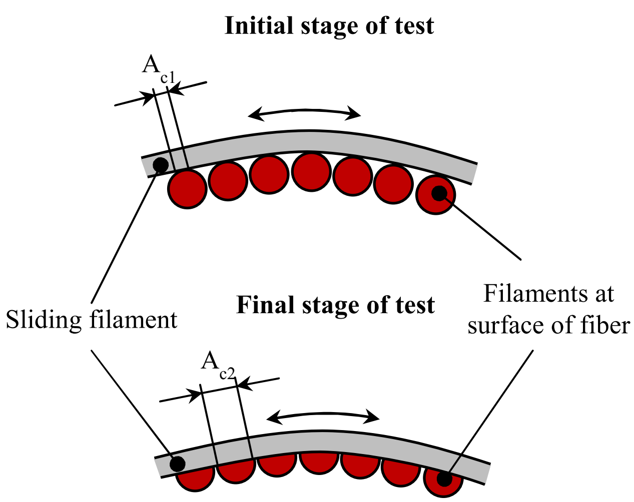

Fig. 20. Hypothesis on the increase in coefficient of friction during cycling: increase of contact area between the sliding filament and the filaments at the surface of the fiber.

At the start of the test, the cross section of the filament transforms from its original circular shape to a flat, ribbon type of shape within a few cycles. This shape does not change significantly during the remainder of the test. The contact width is around 30 µm. During the course of the test, more and more damage is observed in the filaments at the surface of the fiber in contact with the sliding filament (see also Fig. 17). The track increases in depth. This results in an increase in contact area as schematically shown in Fig. 20: the contact area per filament changes from the small area A_{c1} to the larger area A_{c2}. The increase of coefficient of friction occurs in a slower pace for the fiber with XBO finish. For this material it has been observed that the damage to the filaments at the surface of the fiber also occurs at a slower pace.

A more detailed examination has not been performed yet. This may give additional information about the true reasons for the increase in coefficient of friction and the exact reasons for the difference between standard filaments and filaments with XBO finish.

The linear density and tenacity of filaments as determined by the Favimat[4] tester, are shown in Fig. 21 for the standard SK75 filament sliding over standard SK75 fibers and in Fig. 22 for SK75 filaments with XBO finish sliding over SK75 fibers XBO with finish. The linear density is measured by a vibroscopic technique[5][8][13][21].

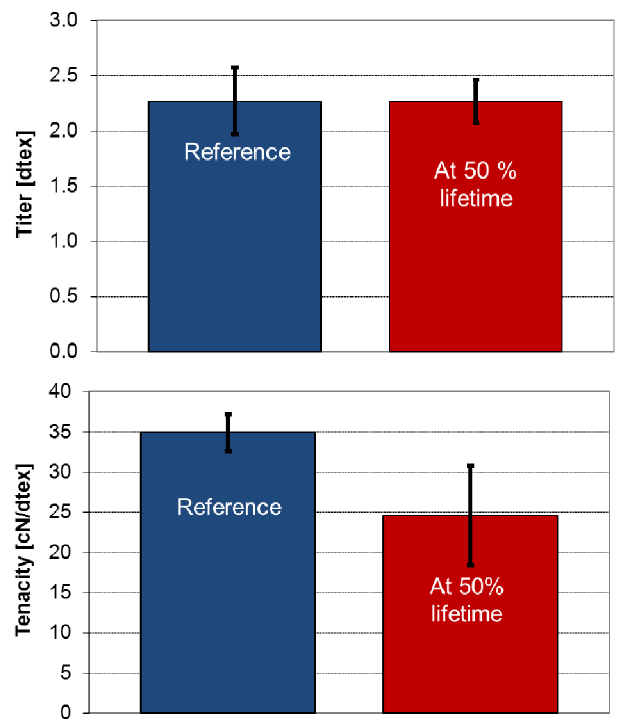

Fig. 21. Linear density and tenacity of standard SK75 filaments sliding over standard SK75 fibers for reference material and after 100 cycles (~50% of the lifetime).

Despite the large scatter on the data, both standard filaments and filaments with XBO finish show a decrease in tenacity during repetitive sliding testing. The linear density of the material however does not decrease. Tests conducted on other types of HMPE filaments at 90% of lifetime and at end of life also showed only a minor reduction of linear density.

The fact that the linear density does not decrease at the same rate as the tenacity is remarkable. The vibroscopic technique measures mass per unit of filament length. The worn off material could still be attached to the filament. The images of filaments at 90% of the lifetime (see Fig. 16) do however not suggest such large amounts of worn material to be present. Possibly, the filament is gradually damaged over its whole volume due to the cyclic shearing/bending action. Another explanation could be that weak points are introduced at the contact surface (crack initiation points), that cause the overall tenacity of the filament to go down. The option of a gradual accumulation of damage in the filament seems the most likely explanation, but it needs further investigations.

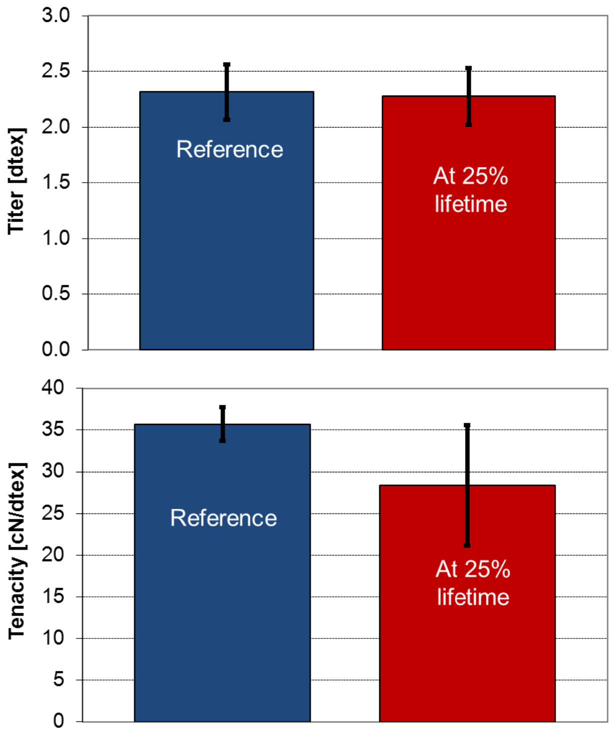

Fig. 22. Linear density and tenacity of SK75 filaments with XBO finish sliding over SK75 fiber with XBO finish for the reference material and after 100 cycles (~ 25% of the lifetime).

IV. Conclusions

Test on braid level and filament level have been conducted for a better understanding of the mechanisms that lead to failure during repetitive bending of HMPE braids. The main locations of failure are the strand cross-over regions, where filaments slide over each other under high contact pressure. Standard braids showed shorter lifetime than braids coated with XBO finish. This is attributed to the adhesion and friction lowering effects of the finish.

The sliding process was investigated in greater detail using a filament friction set up. Filaments with XBO finish have a longer lifetime in this test as well, although there was a large scatter on the data, which is attributed to the variation in the filament properties such as diameter variations and somewhat inhomogenous distribution of the XBO finish over the filament surface. The test also showed a decrease in filament tenacity while, remarkably, the linear density of the filaments did not change, suggesting that a classical wear mechanisms in which material is gradually removed from the contact surface is not occurring. More likely, the combined shearing and bending of the filament introduces damage over the whole volume of the filament.

Future work includes a more in depth (spectroscopic) analysis of the filament at different stages at its lifetime to shed light on the precise damage mechanisms. Furthermore, it is of interest to determine the fundamental loading type (axial tension, lateral/axial shearing) that is responsible for the loss of tenacity of the filaments.

References

[1] J. Cayer-Barrioz, D. Mazuyer, Ph. Kapsa, A. Chateauminois, G. Robert, “Abrasive wear micromechanisms of oriented polymers,” Polymer, vol. 45, pp. 2729–2736, 2004.

[2] J. Cayer-Barrioz, D. Mazuyer, Ph. Kapsa, A. Chateauminois, G. Robert, F. Bouquerel, “On the correlation abrasive wear resistance – molecular weight: a quantitative wear law for polymer fibres,” Wear, vol. 261, pp. 460–466, 2006.

[3] P. Davies, Y. Reaud, L. Dussud, P. Woerther, “Mechanical behavior of HMPE and aramid fibre ropes for deep sea handling operations,” Ocean Engineering, vol. 38, pp. 2208–2214, 2011.

[4] Favimat filament tensile tester, Textechno H.Stein GmbH & Co KG, www.textechno.com.

[5] H. Fletcher, H., “Normal vibration frequencies of a stiff piano string,” The Journal of the Acoustical Society of America, vol. 36, n. 1, pp 203–209, 1964.

[6] J. Gilmore, R. Thomas., “Deepwater synthetic lowering and lifting with enhanced cyclic bend fatigue resistance,” in Deep Offshore Technology Conference, New Orleans, 2008.

[7] M.A. Giordano, S.R. Schmid, “Evaluation of individual fiber wear resistance using accelerated life testing,” Tribology & Lubrication Technology, pp. 44–53, 2012.

[8] W.H. Gloor, Vibroscopic denier determination for high modulus fibers, Technical report AFML-TR-70-151, Air Force Materials Laboratory, 1970.

[9] L. Hoppe, “Performance improvement of Dyneema® in ropes,” in Oceans ’97, MTS/IEEE Conference Proceedings, 1997, pp. 314–318.

[10] J.H. van Leeuwen, A.J. van der Burg, “Bending fatigue behavior of Twaron aramid ropes,” in Proceedings of the Marine Technology Society Conference, 1990, pp. 670–676.

[11] J.H. van Leeuwen, R. Veldhuijzen van Zanten, “Recent Twaron aramid rope developments for dynamic operations,” in Proceedings of the Marine Technology Society Conference, 1991, pp. 835–841.

[12] S. Michielsen, “Tribology in textile manufacturing and use, in Mechanical tribology: materials, characterization, and applications, G.E. Totten, Hong Liang”, Eds. Ch. 11, 2004, pp. 375–395, ISBN 0824748735.

[13] D.J. Montgomery, J.T. Milloway, “The vibroscopic method for determination of fiber cross-sectional area,” Textile Research Journal, vol. 22, pp. 729–735, 1952.

[14] I.C. Roselman, D. Tabor, “The friction and wear of individual carbon fibers,” Journal of Physics, Series D: Applied Physics, vol. 10, pp. 1181–1194, 1977.

[15] A. Sengonul, M.A. Wilding, “Flex fatigue in gel-spun high-performance polyethylene fibres,” Journal of the Textile Institute, vol. 85, n. 1, pp. 1–11, 1994.

[16] A. Sengonul, M.A. Wilding, “Flex fatigue in gel-spun high-performance polyethylene fibres at elevated temperatures,” Journal of the Textile Institute, vol. 87, n. 1, pp. 13–22, 1996.

[17] F. Sloan, R. Nye, T. Liggett, “Improving bend-over-sheave fatigue in fiber ropes,” in Oceans Conference, pp. 1054–1057, 2003.

[18] D. Tabor, “Friction, lubrication and wear of synthetic fibres, Wear, “vol. 1, pp. 5–24, 1957.

[19] W. Vogel, “Dauerbiegeversuche an gedrehten und geflochtenen Faserseilen aus hochfesten Polyethylenfasern,” Technische Textilien, vol. 41, pp. 126–128, 1998.

[20] W. Vogel, “Einfluss de Schlaglänge auf die Lebensdauer laufender hoghfester Faserseile,” EUROSEIL, vol.. 121, n. 3, pp. 57–58, 2002.

[21] E.T.L. Voong, D.J. Montgomery, “Experimental study of stiffness and non-uniformity in the vibroscopic determination of fiber cross-sectional area,” Textile Research Journal, vol. 23, pp. 821–830, 1953.

V. Appendix: Governing Equations for Filament Friction Test

Consider the general case of a filament without bending stiffness sliding over a cylindrical surface with radius R as shown in Fig. 23. The filament slides in counter-clockwise direction and makes first contact with the cylinder at point A and slides off the cylinder again at point B. The tensile force in the filament at point A is T_{in} and at point B T_{out}. The normal force per unit of filament length between the filament and the cylinder is denoted by F_n.

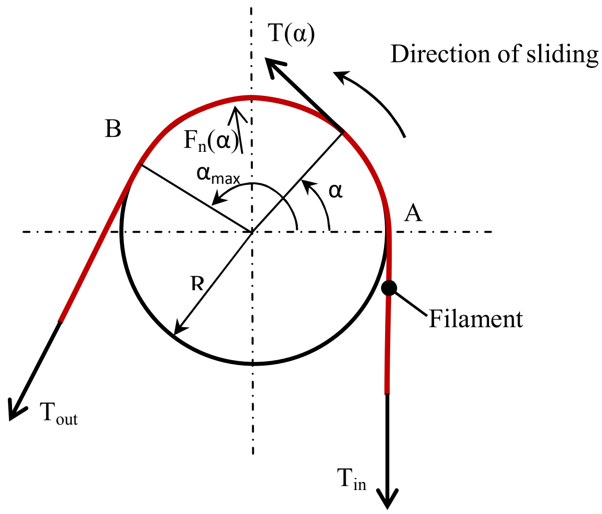

Fig. 23. Single filament without bending stiffness sliding over a cylindrical surface.

If there is no friction between the filament and the cylinder, T_{in} equals T_{out} and the contact normal force F_n is calculated from:

$$F_n(\alpha) = \frac{T}{R} \tag{2}$$

If the contact width between the filament and the cylinder is denoted by w, the average contact pressure follows from:

$$p(\alpha) = \frac{F_n}{w} = \frac{T}{Rw} \tag{3}$$

If there is friction between the filament and the cylinder with constant coefficient of friction μ, T_{out} is greater than T_{in}. The axial tensile force along the filament to cylinder contact varies then according to:

$$T(\alpha) = T_{in} \exp(\mu\alpha). \tag{4}$$

The contact normal force then follows from:

$$F_n(\alpha) = \frac{T_{in}}{R} \exp(\mu\alpha), \tag{5}$$

and the normal pressure from:

$$p(\alpha) = \frac{T_{in}}{Rw} \exp(\mu\alpha) \tag{6}$$

This equation shows that the contact normal pressure increases with contact angle α.

The tensile force T_{out} at the point where the filament leaves the surface (B in Fig. 23), increases exponentially with the maximum contact angle α_{max} (see (4)):

$$T_{out} = T_{in} \exp(\mu\alpha_{max}) \tag{7}$$

If T_{in} and T_{out} are measured in an experiment, this equation can be used to estimate the coefficient of friction μ:

$$\mu = \frac{1}{\alpha_{max}} \ln\left(\frac{T_{out}}{T_{in}}\right) \tag{8}$$